

Oncogenic role of ABHD5 in endometrial cancer

Qing Zhou^{1,2}
Fang Wang³
Kai Zhou¹
Kate Huang³
Qiuyuan Zhu¹
Xishao Luo¹
Jiangtao Yu¹
Zhengzheng Shi¹

¹Department of Gynecology, the First Affiliated Hospital of Wenzhou Medical University, Wenzhou, Zhejiang 325000, P.R. China; ²Department of Obstetrics and Gynecology, Qilu Hospital of Shandong University, Jinan, Shandong 250012, P.R. China; ³Department of Pathology, the First Affiliated Hospital of Wenzhou Medical University, Wenzhou, Zhejiang 325000, P.R. China

Background: Abhydrolase domain containing 5 (ABHD5) functions as a tumor suppressor in colorectal and prostate cancers. The aim of this study was to investigate the roles of ABHD5 in endometrial cancer.

Materials and methods: ABHD5 expression was detected in clinical samples by immunohistochemical staining. Cell proliferation and invasion were evaluated with the Cell Counting Kit-8 and Transwell assay, respectively. Western blotting was performed to analyze protein expression. Glucose uptake was assessed by 2-[N-(7-nitrobenz-2-oxa-1,3-diazol-4-yl)amino]-2-deoxyglucose. Lactate production was detected by a lactate assay kit.

Results: In the present study, ABHD5 was overexpressed in endometrial cancer tissues, and its expression was closely correlated with the International Federation of Gynecology and Obstetrics (FIGO) stage and lymph node metastasis. In addition, we observed that the knockdown of ABHD5 inhibited cell proliferation, invasion, glucose uptake and lactate production in HEC-1A cells, which expressed high levels of ABHD5. Conversely, the opposite effects were observed when ABHD5 was ectopically expressed in Ishikawa cells, which had low levels of ABHD5. Furthermore, the changes in glycolysis regulators (enolase 1 [ENO1], glucose transporter 1 [GLUT1] and lactate dehydrogenase A [LDHA]) and epithelial-to-mesenchymal transition-related proteins (E-cadherin and Snail) in HEC-1A cells with ABHD5 knockdown were consistent with the effects of ABHD5 on glycolysis and cell invasion. Phosphatase and tensin homolog deleted on chromosome 10 (PTEN) was increased, while the phosphorylated AKT (p-AKT) was decreased when ABHD5 was downregulated. Notably, treatment with the allosteric AKT inhibitor MK-2206 completely abolished the effects caused by ABHD5 overexpression in Ishikawa cells. Finally, ABHD5 knockdown potently suppressed tumor growth in vivo.

Conclusion: Overall, these results suggest that ABHD5 may play an oncogenic role in endometrial cancer via the AKT pathway.

Keywords: ABHD5, AKT, endometrial cancer, glycolysis

Introduction

Due to its increasing incidence, endometrial cancer has become the most common gynecologic malignancy of the female reproductive tract in developed countries. Although several risk factors for endometrial cancer, such as older age, obesity, late menopause and infertility, have been proposed,¹ the exact causes of endometrial cancer are still unclear.

Accumulating evidence supports that there is a significant difference in metabolism between cancer cells and normally differentiated cells. In normally differentiated cells, oxidative phosphorylation in the mitochondria provides essential energy, while in rapidly growing cancer cells, aerobic glycolysis provides energy even under aerobic

Correspondence: Zhengzheng Shi;
Jiangtao Yu
Department of Gynecology, The First Affiliated Hospital of Wenzhou Medical University, Nanbaixiang, Ouhai District, Wenzhou, Zhejiang 325000, P.R. China
Email szz19810@163.com;
yjt2005@live.cn

conditions.^{2,3} This phenomenon is known as the Warburg effect, which is characterized by a high rate of glucose uptake and lactate production.⁴ Such metabolic alterations can be essential to sustain the high proliferation rate of cancer cells.² Oncogenes, such as c-Myc⁵ and AKT,⁶ and tumor suppressor genes, including TP53⁷ and phosphatase and tensin homolog deleted on chromosome 10 (PTEN),⁶ are related to high rates of glycolysis and the transcription of genes regulating glycolysis,⁸ such as enolase 1 (ENO1), glucose transporter 1 (GLUT1), lactate dehydrogenase A (LDHA) and pyruvate kinase M2 (PKM2).

Abhydrolase domain containing 5 (ABHD5), also known as comparative gene identification 5 (CGI-58), is an activating coenzyme for adipose triglyceride lipase, which is the rate-limiting enzyme for lipolysis.⁹ In human beings, deficiency of the ABHD5 gene causes Chanarin–Dorfman syndrome, which is an autosomal recessive hereditary disorder of lipid metabolism.^{10,11} Recently, studies have shown the potential functions of ABHD5 in tumorigenesis. Ou et al¹² discovered the tumor-suppressor role of ABHD5 in colorectal cancer. Their results showed that the loss of ABHD5 enhanced aerobic glycolysis and deactivated AMPK/p53 signaling, thus promoting the epithelial-to-mesenchymal transition (EMT). A later report from the same group suggested that ABHD5 showed opposing functions in tumor-associated macrophages,¹³ which indicates that ABHD5 exerts different functions in different cells. A study on prostate cancer also revealed the tumor suppressor role of ABHD5 by preventing EMT and the Warburg effect.¹⁴

In the present study, we explored the expression and function of ABHD5 in endometrial cancer. The AKT pathway was required for the functions of ABHD5 in proliferation, invasion and the Warburg effect.

Materials and methods

Public dataset analysis

The Cancer Genome Atlas (TCGA) endometrial cancer dataset (370 cancer samples and 11 normal uterus tissues) was obtained from cBioportal (www.cbioportal.org). The Mann–Whitney *U* test was used to compare ABHD5 expression between cancer tissues and normal tissues.

Specimen collection

Five paraffin-embedded normal endometrial tissues and 97 paraffin-embedded endometrial adenocarcinoma cancer tissues were obtained from the Department of Obstetrics and Gynecology, Qilu Hospital of Shandong University (Jinan, China). The endometrial cancer specimens were from 97 women who

received a hysterectomy for the removal of endometrial tumors, and normal endometrial tissues were also collected from 5 of these patients as part of the surgical resection. The study was performed in accordance with the Declaration of Helsinki. The use of these clinical materials was approved by the ethics committee of Shandong University and Wenzhou Medical University, and the written informed consent was obtained from all the enrolled participants. The patients with endometrial cancer were staged according to the International Federation of Gynecology and Obstetrics (FIGO) guidelines updated in 2009.

Immunohistochemistry staining

Five-micrometer sections cut from the paraffin blocks were deparaffinized and soaked in 0.3% hydrogen peroxide at room temperature for 15 minutes to block endogenous peroxidase. Heat-mediated antigen retrieval was carried out in 0.01 M citrate buffer (pH 6). Then, a rabbit monoclonal anti-ABHD5 antibody (Abcam, Cambridge, MA, USA) was applied at 4°C overnight. Following incubation with ready-to-use secondary antibodies (Long Island Bio, Shanghai, China), the sections were visualized using a diaminobenzidine kit (Long Island Bio) according to the instruction manual. The slide was counterstained with hematoxylin. The level of ABHD5 staining was evaluated according to the following criteria: a low expression case was determined when 0%–25% of the tumor cells were positively stained, and a high expression case was determined when >25% of the tumor cells were stained.

Cell lines

The human endometrial cancer cell lines, HEC-1A and Ishikawa, were purchased from Cell Bank of Chinese Academy of Sciences (Shanghai, China). HEC-1A cells were maintained in DMEM:nutrient mixture F-12 (DMEM/F-12; HyClone, Logan, UT, USA), and Ishikawa cells were cultured in Roswell Park Memorial Institute-1640 (HyClone). All the media were supplemented with 10% FBS (Thermo Fisher Scientific, Waltham, MA, USA). All the cell lines were cultured in a humidified incubator with 5% CO₂ at 37°C.

RNAi

shRNAs targeting human ABHD5 (shABHD5#1, shABHD5#2 and shABHD5#3) and a negative control (NC) sequence (Table 1) were synthesized by GeneChem Biotech (Shanghai, China) and were inserted into a pLKO.1 vector (Addgene, Cambridge, MA, USA) to make lentiviral constructs. The inserted sequences were confirmed by DNA sequencing. Lentiviral constructs and packaging vectors were cotransfected into 293 T cells with Lipofectamine 2000

Table 1 siRNA sequences for ABHD5

Groups	Sequences
shABHD5#1	5'-GCACCAACAGACCTGTCTA-3'
shABHD5#2	5'-CCAAGTGGTGAGACAGCTT-3'
shABHD5#3	5'-GCAGATCAACCAGAAGAAT-3'
shNC	5'-CCTAAGGTTAAGTCGCCCTCG-3'

(Thermo Fisher Scientific), and ABHD5 shRNA lentiviruses and shNC lentiviruses were collected from the cultured medium at 48–72 hours post transfection.

Plasmids and transient transfection

The ABHD5 coding sequence (CDS) was amplified from human cDNA by PCR with the following primers: 5'-CCCAAGCTTATGGCGGCGGAGGAGGAG-3' and 5'-CCGGAATTCTCAGTCCACAGTGTGCGCAGAT-3', and they were inserted into pcDNA3.1 (Thermo Fisher Scientific) to construct pcDNA3.1-ABHD5. The inserted sequence was confirmed by DNA sequencing. The transfection of plasmids into Ishikawa cells was performed using Lipofectamine 2000 (Thermo Fisher Scientific).

Western blot analysis

Whole-cell protein lysates were prepared with RIPA buffer at 4°C. Standard Western blotting was carried out using whole-cell protein lysates, primary antibodies against ABHD5 (Abcam), E-cadherin (Abcam), Snail (Abcam), ENO1 (Abcam), GLUT1 (Abcam), LDHA (Abcam), phosphorylated AKT (p-AKT; Cell Signaling Technology, Danvers, MA, USA), AKT (Cell Signaling Technology) and a secondary antibody (Beyotime, Shanghai, China). Equal protein loading was ascertained by using an anti-GAPDH antibody (Cell Signaling Technology).

Cell proliferation assay

Cell proliferation was determined by Cell Counting Kit-8 (CCK-8; Dojindo Laboratories, Kumamoto, Japan). Briefly, 3×10^3 cells in 100 μ L of medium were seeded in triplicate in each well of 96-well plates and treated as indicated. Following incubation for 0, 24, 48 and 72 hours, 10 μ L of CCK-8 reagent was added to each well and cultured for another 1 hour. The OD values were measured at 450 nm using a Multiskan MS plate reader (Labsystems, Helsinki, Finland) using wells without cells as blanks.

Cell invasion assay

Cell invasion was assayed using a Transwell chamber with an 8 μ m pore filter (Corning Incorporated, Corning, NY, USA).

Before they were used, the filters were precoated with 1 mg/mL Matrigel. A total of 5×10^4 cells in 300 μ L of serum-free medium was treated as indicated and plated onto the upper chamber, while the lower chamber was filled with 700 μ L of medium containing 10% FBS. The cells were then cultured at 37°C for 24 hours, and nonmigrating cells were completely removed with a cotton swab. Subsequently, the cells that migrated to the bottom of the membrane were fixed in 4% paraformaldehyde and stained with 0.5% crystal violet. The stained cells were observed and counted in five random fields under a microscope, and the average number was calculated.

Measurement of 2-[N-(7-nitrobenz-2-oxa-1,3-diazol-4-yl)amino]-2-deoxyglucose (2-NBDG) uptake

The endometrial cancer cells were treated as indicated for 24 hours, preincubated with glucose-free Krebs–Ringer buffer (KRB) at 37°C for 15 minutes and then incubated with 100 μ M 2-NBDG; Cayman, Ann Arbor, MI, USA) in glucose-free medium (Thermo Fisher Scientific) at 37°C for 45 minutes. After washing with KRB buffer, the fluorescent density was measured using GloMax[®]-Multi+ Detection System (Promega Corporation, Fitchburg, WI, USA) at emission 535 nm and excitation 485 nm. After normalization of the protein content, the values of the control group were set as 100%, and the relative fluorescent density is expressed as the percentage of the control.

Lactate production

The endometrial cancer cells were treated as indicated for 24 hours, and the culture medium was collected to measure lactate production with a lactic acid detection kit (Nanjing Jiancheng Bioengineering Institute, Nanjing, China) according to the manufacturer's protocol.

Tumor growth

The animal experiment was performed in accordance with the guidelines for the Care and Use of Laboratory Animals and was approved by the ethics committee of Wenzhou Medical University. Pathogen-free female athymic nude mice (Shanghai Laboratory Animal Center, Shanghai, China) were randomly divided into two groups (n=6 per group). HEC-1A cells (5×10^6) expressing shABHD5#2 or shNC in 0.1 mL of FBS-free medium were injected subcutaneously into the nude mice. Tumor length and width were monitored every 3 days by caliper measurements after the xenograft formed. Tumor volume was calculated with the following formula: volume = $0.5 \times \text{length} \times \text{width}$.² The mice were sacrificed on day 33

after inoculation, and their tumors were removed, weighed and processed for Western blotting analysis.

Statistical analyses

The GraphPad Prism software program (version 6.0; GraphPad Software, Inc., La Jolla, CA, USA) was used for all statistical analyses. *P*-values of <0.05 were considered statistically significant. A two-tailed chi-squared test and the Fisher’s exact test were used to determine the association between ABHD5 expression and clinical features. The significance of the in vitro and in vivo data was determined using one-way ANOVA or Student’s *t*-test.

Results

Overexpression of ABHD5 in endometrial cancer tissues

To define ABHD5 expression in endometrial cancer, we reanalyzed the gene expression data derived from TCGA dataset. The Mann–Whitney *U* test showed that ABHD5 was significantly overexpressed in endometrial cancer tissues compared with that in normal tissues (*P*<0.0001; Figure 1A). To further verify this finding, we performed immunohistochemistry staining on 5 normal endometrial tissues and 97 endometrial cancer tissues. High expression of ABHD5 was observed in 60 cases of endometrial cancer tissues, which had >25% of tumor cells positively stained, while low expression was observed in the other 37 cases, which had 0%–25% of positively stained tumor cells (Figure 1B). The two-tailed chi-squared test or the Fisher’s exact test indicated that elevated ABHD5 expression was correlated with the FIGO stage and lymph node metastasis but not with patients’ age, histological grade or myometrial invasion (Table 2). The multivariate Cox regression test showed that ABHD5 expression and FIGO stage was independent prognostic factors for endometrial cancer (Table 3).

ABHD5 knockdown suppressed cell proliferation, invasion and the Warburg effect in endometrial cancer cells

Considering that ABHD5 expression was correlated with FIGO stage and lymph node metastasis, we supposed that ABHD5 may affect the proliferation and invasion of endometrial cancer cells. To test this hypothesis, we downregulated ABHD5 expression in HEC-1A cells, which had relatively high levels of ABHD5 (Figure S1), by lentivirus-mediated RNAi (shABHD5#1, shABHD5#2 and shABHD5#3). Figure 2A demonstrates that shABHD5#1, shABHD5#2 and shABHD5#3 effectively downregulated the expression of ABHD5 compared with the control lentivirus (shNC) and control cells without any

Table 2 Correlation of ABHD5 expression with clinicopathological factors in endometrial cancer (n=97)

Variables	All cases	ABHD5		P-value
		Low	High	
Age at surgery (years)				
<60	60	26	34	0.2030
≥60	37	11	26	
Histological grade				
G1	32	14	18	0.3770
G2	39	16	23	
G3	26	7	19	
FIGO stage				
I–II	61	29	32	0.0172*
III	36	8	28	
Lymph node metastasis				
Present	16	2	14	0.0244*
Absent	81	35	46	
Myometrial invasion				
<1/2	63	27	36	0.1933
≥1/2	34	10	24	

Note: **P*<0.05.

Abbreviation: FIGO, International Federation of Gynecology and Obstetrics.

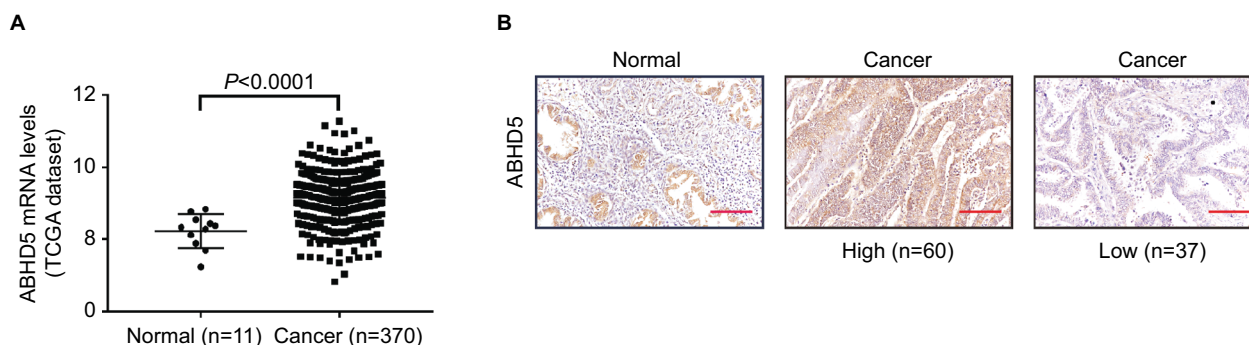


Figure 1 ABHD5 overexpression in endometrial cancer.

Notes: (A) The expression level of ABHD5 in endometrial cancer and normal tissues based on TCGA dataset. (B) Expression of ABHD5 was determined in endometrial cancer tissues and normal tissues by immunohistochemistry staining. Scale bar: 100 μm.

Abbreviation: TCGA, The Cancer Genome Atlas.

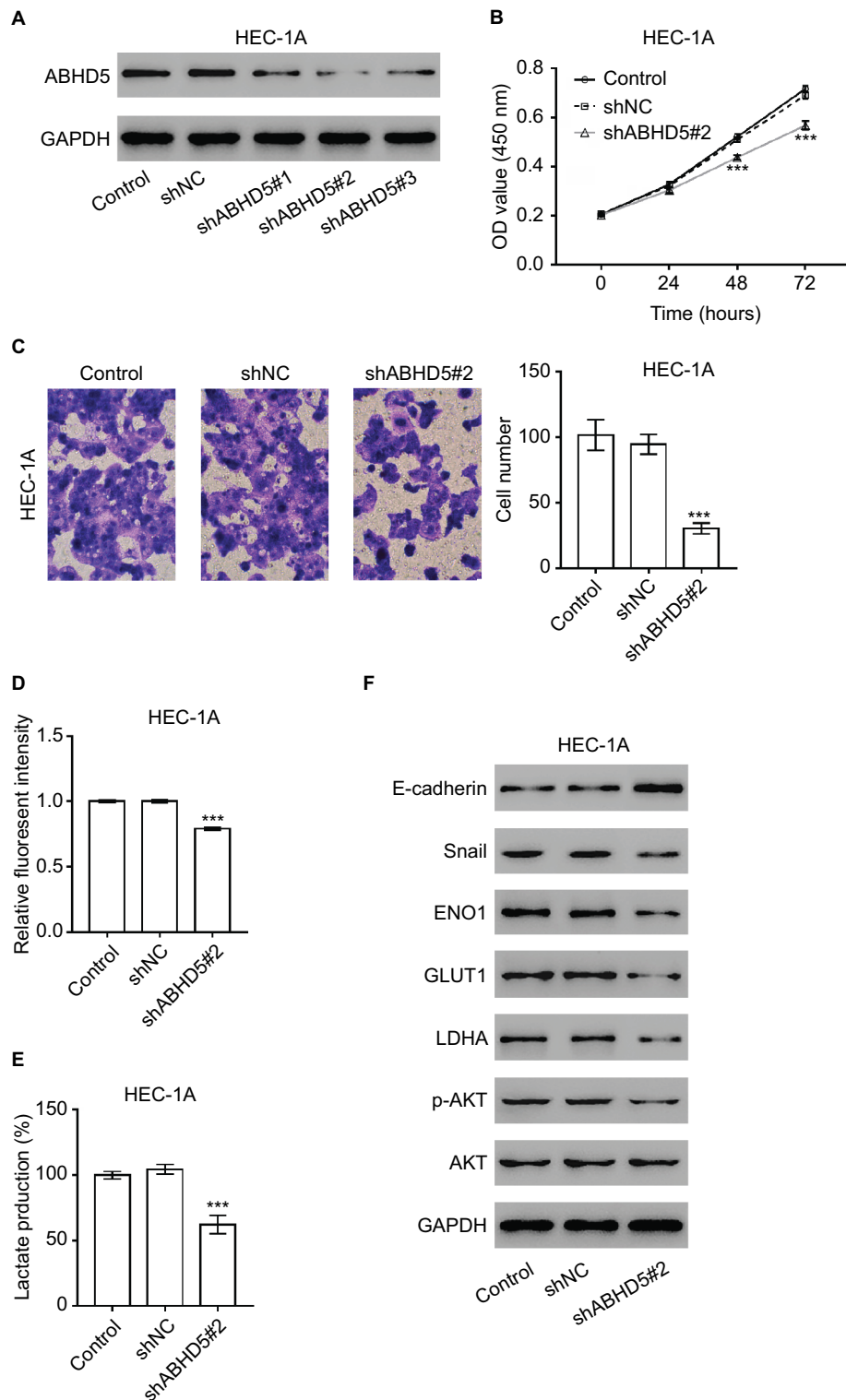


Figure 2 ABHD5 knockdown suppressed endometrial cancer cell proliferation, invasion and the Warburg effect.

Notes: (A) HEC-1A cells were transfected with ABHD5 shRNA and control shRNA (shNC). Cells without any treatment served as a control. Western blot analysis was performed to evaluate the efficiency of three ABHD5 shRNAs in HEC-1A cells at 48 hours post treatment. Representative blots from three independent experiments are shown. (B) Cell proliferation was determined by CCK-8 assay (n=3 biological replicates) in HEC-1A cells transfected with shABHD5#2 and shNC. (C) A Transwell assay (n=3 biological replicates) was performed to assess cell invasive ability, magnification 200 \times . (D) 2-NBDG uptake was measured (n=3 biological replicates) at 24 hours post treatment. Fluorescent intensity was normalized to protein content and then divided by the value of the control. (E) Lactate production (n=3 biological replicates) was measured and divided by the value of the control. (F) Western blot analysis was performed to detect the related proteins. Representative blots from three independent experiments are shown. ***P<0.001 vs the control and shNC.

Abbreviations: 2-NBDG, 2-[N-(7-nitrobenz-2-oxa-1,3-diazol-4-yl) amino]-2-deoxyglucose; CCK-8, Cell Counting Kit-8.

treatment. We found significant decreases in cell proliferation (Figure 2B) and invasion (Figure 2C) of HEC-1A cells with ABHD5 knockdown (shABHD5#2). In comparison, ABHD5 overexpression (Figure S2A) markedly increased cell proliferation (Figure S2B) and invasion (Figure S2C) in Ishikawa cells, which had relatively low levels of ABHD5 (Figure S1).

Given that the Warburg effect provides energy for cancer cell proliferation and invasion,² we detected the changes in glucose uptake and lactate production. Significant decreases in 2-NBDG uptake (Figure 2D) and lactate production (Figure 2E) were observed in HEC-1A cells with ABHD5 knockdown. In comparison, ABHD5 overexpression showed opposite effects in Ishikawa cells (Figures S2D and S2E).

Oncogenes such as c-Myc⁵ and AKT,⁶ tumor suppressor genes such as TP53⁷ and PTEN,⁶ regulators of oxygen homeostasis such as HIF1A³ and glycolysis genes such as ENO1, GLUT1, LDHA and PKM2⁸ play a critical role in regulating cell glycolysis. Real-time PCR showed that ABHD5 knockdown caused a reduction in the mRNA levels of ENO1, GLUT1

and LDHA and an increase in PTEN (Table S1 and Figure S3). Western blotting was then performed, and it validated the most significantly changed genes: PTEN, ENO1, GLUT1 and LDHA (Figure 2F). The p-AKT was also reduced with the knockdown of ABHD5 (Figure 2F). Moreover, consistent with the effects of ABHD5 on cell invasion, ABHD5 knockdown caused a significant increase in E-cadherin protein expression but a decrease in the protein levels of Snail (Figure 2F).

Activation of the AKT pathway is necessary for the biological functions of ABHD5 in endometrial cancer cells

To corroborate the role of AKT activation in the biological functions of ABHD5 in endometrial cancer cells, Ishikawa cells were overexpressed with ABHD5 and treated with a specific inhibitor of the AKT pathway (MK-2206). Notably, treatment with MK-2206 (10 μ M) completely abolished the ABHD5 overexpression-stimulated proliferation (Figure 3A), invasion (Figure 3B), glucose consumption (Figure 3C) and

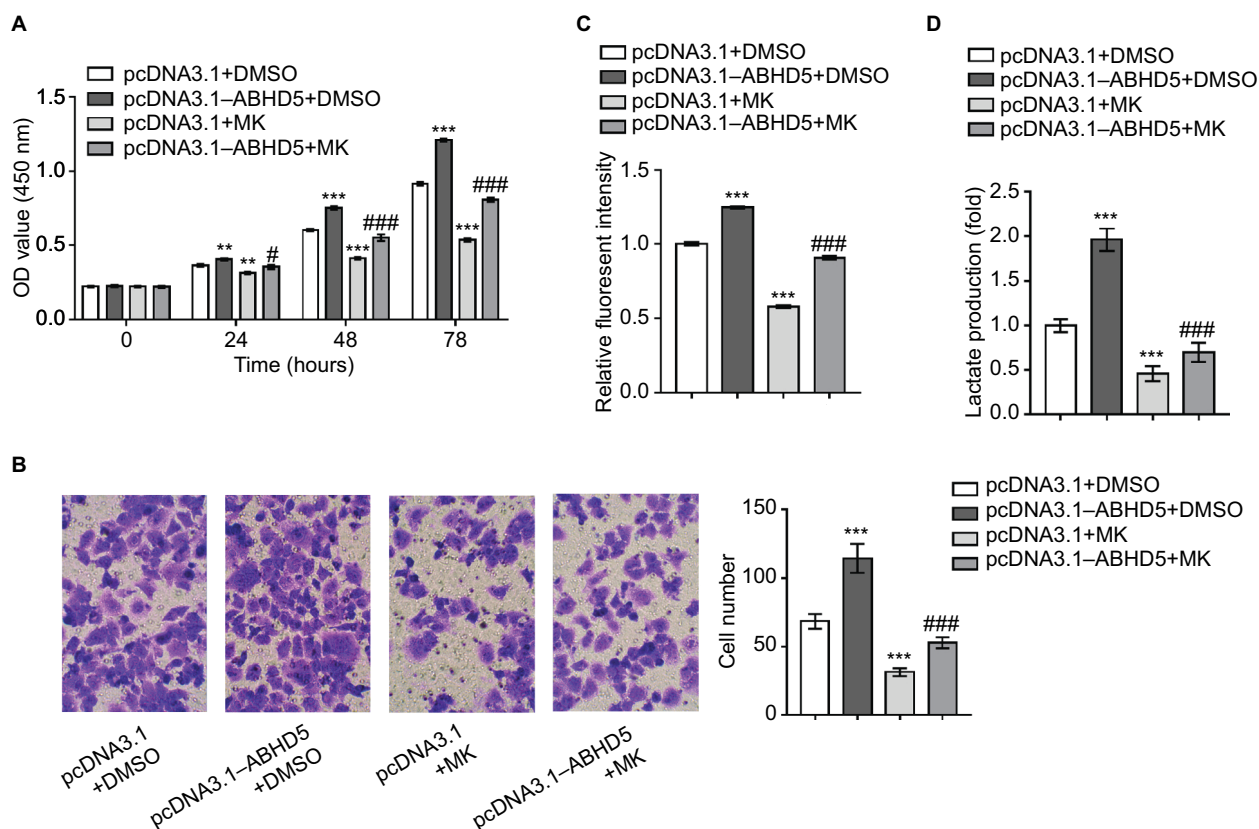


Figure 3 The activation of AKT is necessary for the biological functions of ABHD5 in endometrial cancer cells.

Notes: Ishikawa cells were transfected with pcDNA3.1-ABHD5 or pcDNA3.1 and treated with 10 μ M MK-2206 (MK; Merck Millipore, Billerica, MA, USA) or vehicle (DMSO). (A) Cell proliferation was detected by CCK-8 assay (n=3 biological replicates). (B) Cell invasion was detected by Transwell assay (n=3 biological replicates), magnification 200 \times . (C) 2-NBDG uptake was measured (n=3 biological replicates). Fluorescent intensity was normalized to protein content and then divided by the value of the control (the first column). (D) Lactate production (n=3 biological replicates) was measured and divided by the value of the control (the first column). ** P <0.01, *** P <0.001 vs pcDNA3.1+DMSO; # P <0.05, ### P <0.001 vs pcDNA3.1+MK.

Abbreviations: 2-NBDG, 2-[N-(7-nitrobenz-2-oxa-1,3-diazol-4-yl) amino]-2-deoxyglucose; CCK-8, Cell Counting Kit-8; DMSO, dimethylsulfoxide; MK, MK-2206.

lactate production (Figure 3D) in Ishikawa cells. These data suggested that the AKT pathway was required for the effects of ABHD5 in endometrial cancer cells.

Impact of ABHD5 knockdown on endometrial cancer growth in vivo

To determine the direct effect of ABHD5 on endometrial cancer biology, we evaluated the ability of HEC-1A cells with ABHD5 knockdown to grow in nude mice. The tumor growth curve results as shown in Figure 4A demonstrate that the growth rate of xenografts formed from cells with shABHD5#2 was markedly slower than that from cells with shNC. On day 33, the weight of the shABHD5#2 xenografts was significantly lower than that of shNC xenografts (Figure 4B). The Western blotting results as shown in Figure 3C

demonstrate the reduced expression of ABHD5, Snail, ENO1, GLUT1, LDHA and p-AKT and the elevated expression of E-cadherin and PTEN in shABHD5#2 xenografts, which were in line with the in vitro data.

Discussion

ABHD5 was reported to play a tumor-suppressive role in colorectal cancer¹² and prostate cancer.¹⁴ However, we demonstrated that ABHD5 is highly expressed in endometrial cancer. In vitro cellular experiments and an in vivo xenograft model suggest that ABHD5 is an oncogene in endometrial cancer development and progression. This finding may not be surprising, because a previous study suggested the presence of ABHD5 in tumor-associated macrophages, suggesting that ABHD5 exerts different functions in different cells.¹³

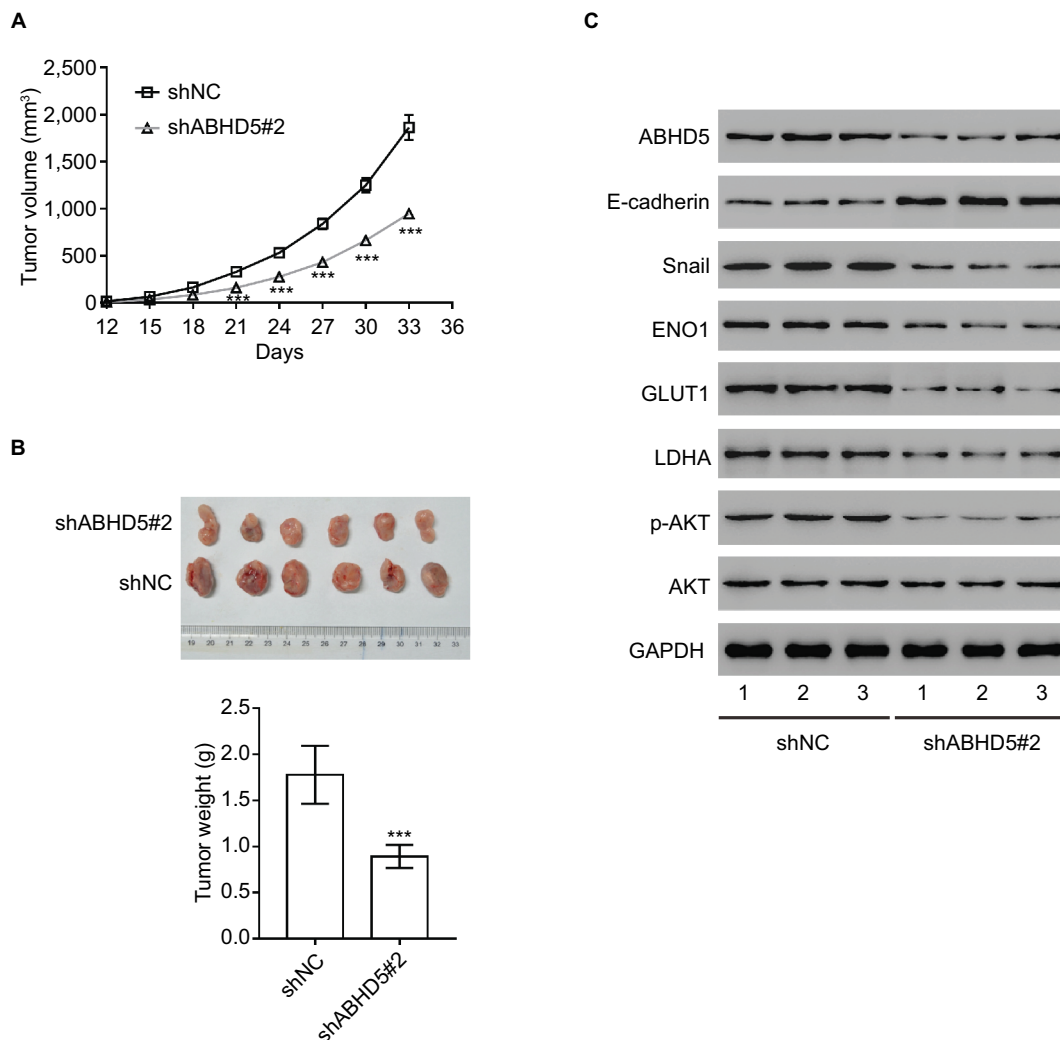


Figure 4 Impact of ABHD5 knockdown on endometrial cancer growth in vivo.

Notes: (A, B) ABHD5 knockdown significantly blocked xenograft growth in nude mice (n=6 per group). Tumor volume was measured every 3 days. On day 33 after inoculation, the mice were sacrificed and tumors were weighed (n=6). (C) Western blotting was performed to assess the expression of the indicated proteins in xenografts. Representative blots from three independent experiments are shown. ***P<0.001.

Table 3 Multivariate Cox regression of prognostic parameters for survival in patients with endometrial cancer

Prognostic parameters	Multivariate analysis		
	HR	95% CI	P-value
Expression of ABHD5 (low vs high)	13.782	4.087–46.476	<0.001
FIGO stage (I/II vs III)	46.196	11.972–178.255	<0.001
Lymph node metastasis (present vs absent)	0.628	0.254–1.556	0.315

Abbreviation: FIGO, International Federation of Gynecology and Obstetrics.

In the current study, we demonstrated that elevated expression of ABHD5 is significantly correlated with FIGO stage and lymph node metastasis in endometrial cancer (Table 2). In line with these findings, in clinical samples, we found that ABHD5 knockdown in endometrial cancer cells blocked cell proliferation and invasion as indicated by CCK-8 (Figure 2B) and Transwell assays (Figure 2C). Moreover, during the invasion process, EMT occurs in epithelial tumor cells, which is characterized by the loss of E-cadherin and the induction of the transcriptional repressors for E-cadherin.^{15,16} As expected, the suppressed invasive ability of endometrial cancer cells with ABHD5 knockdown was associated with an increase in E-cadherin and a reduction in Snail, a transcriptional suppressor for E-cadherin (Figure 2F). These data imply that ABHD5 may affect endometrial cancer cell invasion by regulating EMT transition. Furthermore, the Warburg effect, which provides energy for cancer cell proliferation and invasion,² was reduced by ABHD5 knockdown, as indicated by decreased glucose uptake and lactate production. The expression of glycolysis genes, including ENO1, GLUT1 and LDHA,⁸ was also reduced in ABHD5 knockdown cells, which further confirmed the reduction in the Warburg effect.

The phosphatidylinositol-3-kinase (PI3K)/AKT pathway has been regarded as an important regulator of copious cellular processes including survival, proliferation, invasion, metabolism and angiogenesis. PTEN dephosphorylates phosphatidylinositol-3,4,5-trisphosphate to form inactive phosphatidylinositol-4,5-bisphosphate, thereby antagonizing the effect of PI3K and suppressing AKT activation.¹⁷ Loss-of-function mutations of PTEN have frequently been observed in endometrial cancer. MK-2206, an allosteric AKT inhibitor, showed antitumor activity in various cancer cell lines, including endometrial cancer cells.¹⁸ PTEN and AKT⁶ are critically related to the high glycolysis rate of cancer cells. In the current study, ABHD5 knockdown decreased the p-AKT in both endometrial cancer cells (Figure 2F) and xenografts (Figure 4C). Thus, we propose that AKT activa-

tion is required for the biological functions of ABHD5 in endometrial cancer cells. The AKT inhibitor MK-2206 can block the increased cell proliferation, invasion, glucose uptake and lactate production caused by ABHD5 overexpression (Figure 3). These data suggest that ABHD5 may play an oncogenic role in endometrial cancer through the AKT signaling pathway.

Conclusion

Our study revealed that ABHD5 could promote cell proliferation and invasion and could enhance the Warburg effect in endometrial cancer cells through the AKT signaling pathway. These findings suggest that ABHD5 can act as a potential therapeutic target in endometrial cancer.

Acknowledgment

This study was supported by a grant from Wenzhou Science and Technology Planning Project (project number: Y20180272).

Disclosure

The authors report no conflicts of interest in this work.

References

1. Ali AT. Risk factors for endometrial cancer. *Ceska Gynekol*. 2013;78(5):448–459.
2. Vander Heiden MG, Cantley LC, Thompson CB. Understanding the Warburg effect: the metabolic requirements of cell proliferation. *Science*. 2009;324(5930):1029–1033.
3. Koppenol WH, Bounds PL, Dang CV. Otto Warburg's contributions to current concepts of cancer metabolism. *Nat Rev Cancer*. 2011;11(5):325–337.
4. Bayley JP, Devilee P. The Warburg effect in 2012. *Curr Opin Oncol*. 2012;24(1):62–67.
5. Dang CV, Le A, Gao P. Myc-induced cancer cell energy metabolism and therapeutic opportunities. *Clin Cancer Res*. 2009;15(21):6479–6483.
6. Cairns RA, Harris IS, Mak TW. Regulation of cancer cell metabolism. *Nat Rev Cancer*. 2011;11(2):85–95.
7. Puzio-Kuter AM. The role of p53 in metabolic regulation. *Genes Cancer*. 2011;2(4):385–391.
8. Doherty JR, Cleveland JL. Targeting lactate metabolism for cancer therapeutics. *J Clin Invest*. 2013;123(9):3685–3692.
9. Zechner R. FAT FLUX: enzymes, regulators, and pathophysiology of intracellular lipolysis. *EMBO Mol Med*. 2015;7(4):359–362.
10. Lass A, Zimmermann R, Haemmerle G, et al. Adipose triglyceride lipase-mediated lipolysis of cellular fat stores is activated by CGI-58 and defective in Chanarin-Dorfman syndrome. *Cell Metab*. 2006;3(5):309–319.
11. Yamaguchi T, Osumi T. Chanarin-Dorfman syndrome: deficiency in CGI-58, a lipid droplet-bound coactivator of lipase. *Biochim Biophys Acta*. 2009;1791(6):519–523.
12. Ou J, Miao H, Ma Y, et al. Loss of ABHD5 promotes colorectal tumor development and progression by inducing aerobic glycolysis and epithelial-mesenchymal transition. *Cell Rep*. 2014;9(5):1798–1811.
13. Miao H, Ou J, Peng Y, et al. Macrophage ABHD5 promotes colorectal cancer growth by suppressing spermidine production by SRM. *Nat Commun*. 2016;7(1):11716.

14. Chen G, Zhou G, Aras S, et al. Loss of ABHD5 promotes the aggressiveness of prostate cancer cells. *Sci Rep.* 2017;7(1):13021.
15. Tanaka Y, Terai Y, Kawaguchi H, et al. Prognostic impact of EMT (epithelial-mesenchymal-transition)-related protein expression in endometrial cancer. *Cancer Biol Ther.* 2013;14(1):13–19.
16. Yeramian A, Moreno-Bueno G, Dolcet X, et al. Endometrial carcinoma: molecular alterations involved in tumor development and progression. *Oncogene.* 2013;32(4):403–413.
17. Martini M, De Santis MC, Braccini L, Gulluni F, Hirsch E. PI3K/Akt signaling pathway and cancer: an updated review. *Ann Med.* 2014;46(6):372–383.
18. Hirai H, Sootome H, Nakatsuru Y, et al. MK-2206, an allosteric Akt inhibitor, enhances antitumor efficacy by standard chemotherapeutic agents or molecular targeted drugs in vitro and in vivo. *Mol Cancer Ther.* 2010;9(7):1956–1967.

Supplementary materials

Materials and methods

The human endometrial cancer cell lines, RL952 and AN3CA, were purchased from Cell Bank of Chinese Academy of Sciences (Shanghai, China). RL952 cells were maintained in DMEM:nutrient mixture F-12 (DMEM/F-1; HyClone, Logan, UT, USA), and AN3CA cells were cultured in DMEM (HyClone). All the media were supplemented with 10% FBS (Thermo Fisher Scientific, Waltham, MA, USA). All the cell lines were cultured in a humidified incubator with 5% CO₂ at 37°C.

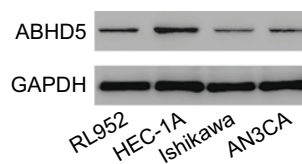


Figure S1 ABHD5 expression level in four endometrial cancer cell lines was analyzed by Western blot.

Note: Representative blots from three independent experiments are shown.

Table S1 Primer sequences

Gene	Primers
c-Myc	Forward 5'-CCTTCTTTCTCCACTCTC-3' Reverse 5'-CAAACCCTCTCCCTTTCTC-3'
PTEN	Forward 5'-GATGTGGCGGGACTCTTTATG-3' Reverse 5'-AGCGGCTCAACTCTCAAAC-3'
TP53	Forward 5'-GTGAGGGATGTTTGGGAGATG-3' Reverse 5'-CCTGGTTAGTACGGTGAAGTG-3'
HIF1A	Forward 5'-CTGGCTACAATACTGCACAAAC-3' Reverse 5'-ATGCTACTGCAATGCAATGG-3'
ENO1	Forward 5'-AACTGCCTCCTGCTCAAAGTC-3' Reverse 5'-TGCCCAGCTCCTCTTCAATTC-3'
LDHA	Forward 5'-CCTGTATGGAGTGAATG-3' Reverse 5'-GGATGTGTAGCCTTTGAG-3'
GLUT1	Forward 5'-TCACTGTGCTCCTGGTTCTG-3' Reverse 5'-CGGGTGTCTTGCACTTTGG-3'
PKM2	Forward 5'-AGCAAGAAGGGTGTGAAC-3' Reverse 5'-CGGATGAATGACGCAAAC-3'
GAPDH	Forward 5'-AATCCCATCACCATCTTC-3' Reverse 5'-AGGCTGTTGCATACTTC-3'

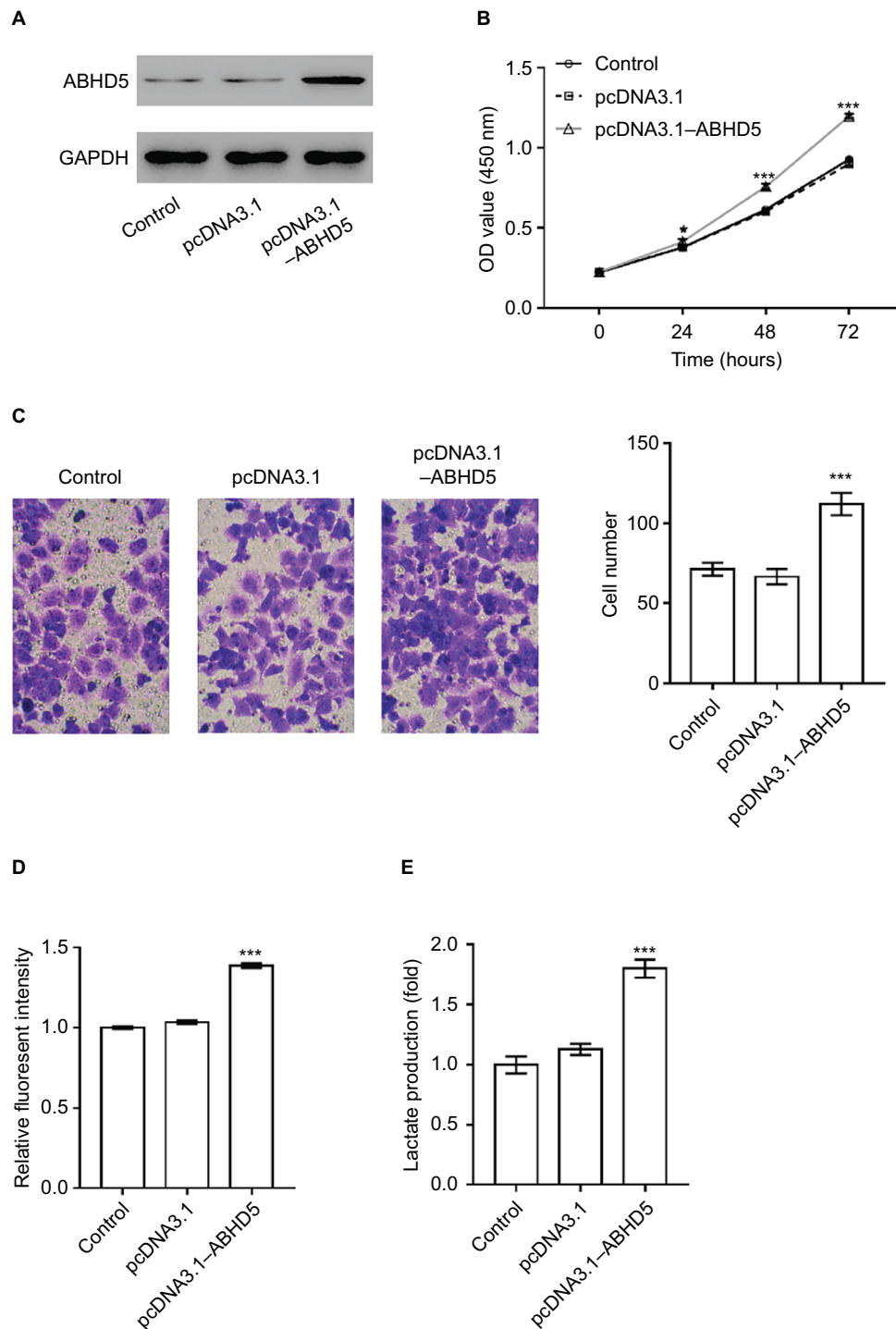


Figure S2 ABHD5 overexpression promoted endometrial cancer cell proliferation, invasion and the Warburg effects.

Notes: (A) Ishikawa cells were transfected with pcDNA3.1-ABHD5 or pcDNA3.1. Cells without any treatment were served as control. Western blot was performed to evaluate ABHD5 expression. Representative blots from three independent experiments are shown. (B) Cell proliferation was assessed by CCK-8 assay (n=3 biological replicates) in Ishikawa cells with pcDNA3.1-ABHD5 or pcDNA3.1. (C) Transwell assay (n=3 biological replicates) was performed to assess cell invasive ability, magnification 200 \times . (D) 2-NBDG uptake was measured (n=3 biological replicates) at 24 hours post treatment. Fluorescent intensity was normalized to protein content and then divided to the value of control. (E) Lactate production (n=3 biological replicates) was measured and divided to the value of control. * $P < 0.05$, *** $P < 0.001$ vs control and shNC.

Abbreviations: 2-NBDG, 2-[N-(7-nitrobenz-2-oxa-1,3-diazol-4-yl) amino]-2-deoxyglucose; CCK-8, Cell Counting Kit-8.

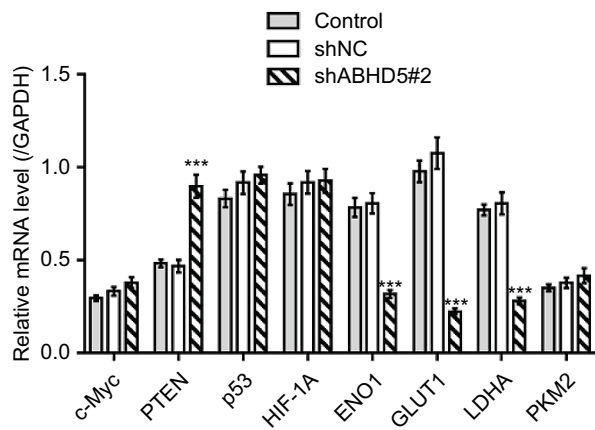


Figure S3 mRNA expression of related genes (n=3 biological replicates).

Notes: HEC-1A cells were transduced with ABHD5 shRNA and control shRNA (shNC). Cells without any treatment were served as control. *** $P < 0.001$ vs control and shNC.

Cancer Management and Research

Publish your work in this journal

Cancer Management and Research is an international, peer-reviewed open access journal focusing on cancer research and the optimal use of preventative and integrated treatment interventions to achieve improved outcomes, enhanced survival and quality of life for the cancer patient. The manuscript management system is completely online and includes

Submit your manuscript here: <https://www.dovepress.com/cancer-management-and-research-journal>

Dovepress

a very quick and fair peer-review system, which is all easy to use. Visit <http://www.dovepress.com/testimonials.php> to read real quotes from published authors.